Proceedings of Ninth World Conference on Earthquake Engineering
August 2-9, 1988, Tokyo-Kyoto, JAPAN (Vol.II)

2-1-13

A PROBABILISTIC MODEL FOR SEISMIC HAZARD ESTIMATION IN THE KANTO DISTRICT

Tadashi ANNAKA[1] and Yoshiyuki NOZAWA[2]

[1]Seismic Engineering Department, Tokyo Electric Power Services Co.,Ltd., Chiyoda-ku, Tokyo, Japan
[2]Engineering Research Center, Tokyo Electric Power Co.,Inc., Chofu-city, Tokyo, Japan

SUMMARY

A probabilistic model for seismic hazard estimation in the Kanto district was proposed. Seismic source zones were defined in three dimensional space based on the regional plate tectonics and seismicity. The occurrence of earthquakes in the seismic source zones was described by either a characteristic earthquake model or a b-value model. Attenuation equations were derived using the data collected by TEPCO's network. The effect of focal depths is incorporated into the attenuation equations. The effect of fault extent and the recurrence nature of large earthquakes can be included. Examples calculated from the model were shown.

INTRODUCTION

The objective of the present study is to develop a probabilistic model for seismic hazard estimation in the Kanto district, Japan, more realistically. There exist two types of earthquakes that caused severe damage in the Kanto district. One is the large earthquakes (magnitude M>7.5) occurred along the plate boundaries. The rupture zone of the large interplate earthquake is so large that it is necessary to use a finite-fault rupture model for seismic hazard estimation. The other is the moderate earthquakes (M≈7.0) occurred in the crust and the uppermost mantle beneath the district. The damage patterns of the moderate earthquakes are very sensitive to their focal depths when their magnitudes are nearly equal. For example, the damage of the 1855 Ansei-Edo earthquake (M=6.9) is much greater than that of the 1894 Tokyo earthquake (M=7.0). Therefore it is important to incorporate focal depths into seismic hazard estimation.

EARTHQUAKE OCCURRENCE MODEL

Seismic Source Zones The nature of seismic activity is assumed to be uniform in a seismic source zone, which is represented by a rectangular plane in three dimensional space in this study. We defined seismic source zones as shown in Fig.1 based on the regional plate tectonics and seismicity. The seismic source zones were divided into two groups by the difference of earthquake occurrence models. The occurrence of earthquakes in the seismic source zones where the large "characteristic" earthquakes occurred periodically was described by a characteristic earthquake model (Refs.1,2). Figure 1(a) shows the seismic source zones for the characteristic earthquake model. The distribution of magnitudes was assumed to be uniform in a narrow range. The return period of characteristic earthquakes for each zone was decided from previous studies about historical earthquakes and

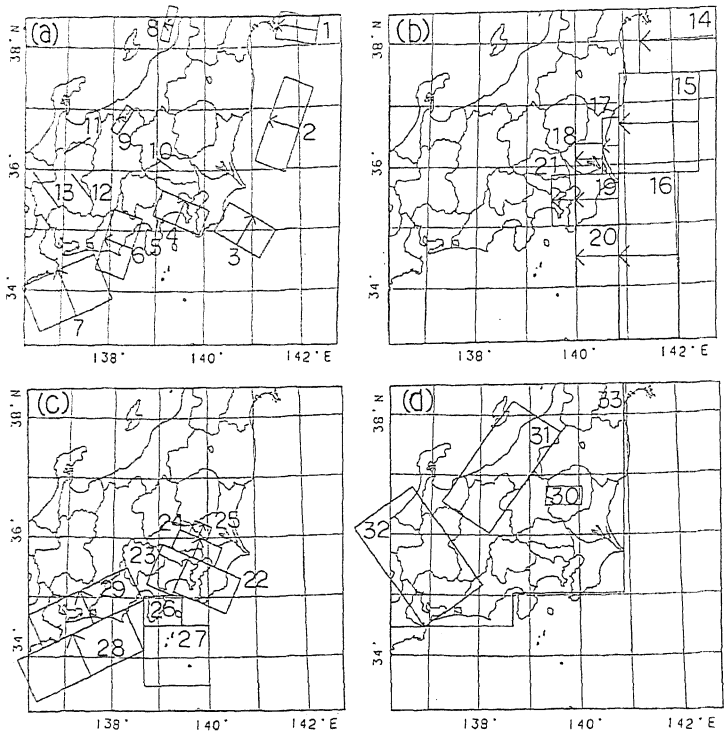

Fig.1 Distribution of seismic source zones : (a) zones for the large earthquakes, (b) zones on the upper plane of the Pacific plate, (c) zones on the upper plane of the Philippine Sea plate, (d) zones on the horizontal plane in the Continental plate. Arrows denote the dip direction of the zone.

active faults. Each seismic source zone of this type consists of a single fault. The occurrence of earthquakes in other seismic source zones that include many small faults was described by a b-value model (Ref.2). The distribution of magnitudes was given by the truncated Gutenberg-Richter relationship

$$\log N = a - bM \qquad (1)$$

where N is the annual number of earthquakes with magnitude greater than or equal to M. The seismic source zones for the b-value model were distributed on and near three planes : the upper plane of the Pacific plate (Fig.1(b)), that of the Philippine Sea plate (Fig.1(c)), and the horizontal plane with a depth of 5km in the Continental plate (Fig.1(d)). The partition was made based on the difference of seismicity. The coefficient b was assumed to be constant for all zones and estimated to be 1.0 from the data of the whole area shown in Fig.1. The coefficient a for each zone was determined from the number of earthquakes with magnitude greater than or equal to 6.0 during the period between 1885 and 1986. The minimum magnitude was 5.5 except zone 30 where few earthquakes with magnitude between 5.5 and 5.9 occurred during the last 102 years. The maximum magnitude for each zone was estimated from the historical earthquake data. The occurrence of larger earthquakes in zone 26 was described by the characteristic earthquake model because the gap exists in the magnitude distribution.

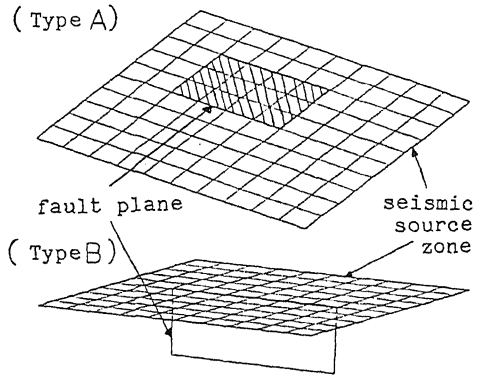

Fig.2 Schematic diagram for explaining two types of finite fault models : (upper) Type A, (lower) Type B.

Finite Fault Model The Blume's method (Ref.3) for a line source was extended

for a plane source. Figure 2 shows a schematic diagram which explains the method for the plane source. The plane of the seismic source zone is divided into small elements in order to make the number of fault locations finite. The size of the small element used in this study was 5km × 5km. Two types were assumed on the relation between fault plane and zone plane. For type A, fault plane is placed on zone plane. For type B, fault plane is perpendicular to zone plane and two cases were assumed on the strike of fault. For type B-1, the strike is fixed in only one direction. For type B-2, the strike is in two directions which are perpendicular each other. The point source model (Type C) was applied for the seismic source zones where the relation between fault plane and zone plane is not clear. The parameters for the seismic source zones are listed in Table 1. In this study fault length, L(km), and width, W(km), were determined from magnitude, M, using the relations

$$\log L = 0.5M - 2.044$$
$$L = 2W. \qquad (2)$$

Stochastic Time Predictable Model We used a stochastic time predictable model (Ref.4) for evaluating instantaneous seismic hazard. In this study we applied the model for three seismic source zones of numbers 4,6 and 7. The parameters of the Weibull distribution were determined from a mean return period and a coefficient of variation. The mean return period for each magnitude was estimated from that for a reference magnitude by assuming that a slip rate is constant. The relation between magnitude, M, and coseismic displacement, d, was assumed as

$$d \propto 10^{0.5M}. \qquad (3)$$

The parameters of the model used in the calculation are listed in Table 2. The magnitude of the latest earthquake was assumed to be the same as the reference magnitude. Figure 3 shows the expected number of earthquakes from the present

Table 1 Parameters for seismic source zones.

ZONE NUMBER	LENGTH KM	WIDTH KM	DEPTH OF TOP KM	DIP ANGLE DEG	MAGNITUDE RANGE	RETURN PERIOD YEAR	a	b	TYPE OF SOURCE
1	50	80	25	20	7.4-7.6	40	-	-	A
2	160	60	20	10	7.8-8.1	1000	-	-	A
3	100	70	2	30	7.9-8.2	1000	-	-	A
4	95	54	2	25	7.9-8.2	200	-	-	A
5	30	10	0	90	7.0-7.3	1000	-	-	A
6	115	70	2	34	7.9-8.4	130	-	-	A
7	150	100	3	24	7.9-8.4	130	-	-	A
8	65	30	0	56	7.4-7.6	500	-	-	A
9	55	30	0	56	7.3-7.5	500	-	-	A
10	40	10	1	90	6.8-7.0	1500	-	-	A
11	60	15	0	90	7.7-7.8	1000	-	-	A
12	65	15	0	90	7.7-7.8	1000	-	-	A
13	80	15	0	90	7.9-8.0	1000	-	-	A
14	115	145	20	16	5.5-7.5	-	5.7	1.0	A
15	180	150	10	12	5.5-7.5	-	6.0	1.0	A
16	305	115	0	20	5.5-7.5	-	5.5	1.0	A
17	100	30	40	18	5.5-6.5	-	4.3	1.0	B-1
18	55	55	30	22	5.5-7.2	-	4.9	1.0	B-1
19	95	85	40	21	5.5-6.5	-	5.1	1.0	B-1
20	110	85	40	21	5.5-6.5	-	4.8	1.0	B-1
21	95	45	70	13	5.5-7.1	-	4.6	1.0	B-1
22	105	75	20	0	5.5-7.0	-	4.9	1.0	A
23	55	80	20	0	5.5-7.3	-	5.0	1.0	A
24	85	45	20	28	5.5-7.1	-	4.3	1.0	A
25	35	25	40	22	5.5-6.1	-	4.5	1.0	A
26-1	75	55	5	0	6.7-7.0	34	-	-	C
26-2	75	55	5	0	5.5-6.1		4.4	1.0	C
27	125	110	5	0	5.5-6.8	-	5.2	1.0	C
28	225	90	0	13	5.5-7.0	-	4.0	1.0	A
29	210	70	20	17	5.5-6.4	-	4.6	1.0	A
30	65	35	5	0	6.0-7.3	-	4.5	1.0	A
31	225	105	5	0	5.5-7.0	-	4.9	1.0	B-1
32	225	130	5	0	5.5-7.4	-	5.2	1.0	B-2
33	-	-	5	0	5.5-6.5	-	4.6	1.0	C

Table 2 Parameters of the stochastic time-predictable model.

N	MR	TR	Cv	T
4	8.0	200	0.10	1923
6	8.1	130	0.18	1854
7	8.1	130	0.18	1944

N ; zone Number, MR ; reference magnitude, TR ; mean return period (yr.) for MR , Cv ; coefficient of variation, T ; time (A.D.) when the latest earthquake occurred.

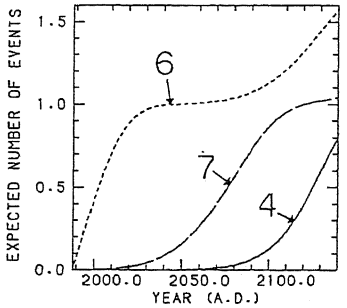

Fig.3 Expected number of earthquakes as a function of time obtained from the stochastic time-predictable model. Numbers denote the seismic source zone in Fig.1.

(A.D.1988) to A.D.2140 for three zones. In zone 6 a large earthquake is expected to occur in the near future.

ATTENUATION MODEL

We derived attenuation equations for peak horizontal ground motions and acceleration response spectra using the data collected by TEPCO's network. The acceleration records were obtained for 45 earthquakes with focal depth less than 100km during the period from 1971 to 1986. The observed motions obtained at the ground surface where S wave velocity (Vs) is less than 300m/s were converted into the incident motions at the base layer where Vs is greater than 300m/s, using one-dimensional wave propagation theory. The acceleration time histories were integrated to obtain those of velocity and displacement.

We fitted the data by multiple linear regression using the equations

$$\log A = CmM + ChH - Cd \log D + Co + CpP$$
$$D = R + 0.35 \exp(0.65M) \qquad (4)$$

where A is the intensity of ground motion (peak ground acceleration (PGA), velocity and displacement and acceleration response spectra), M is magnitude, H is the depth of the point on the fault plane in km when R becomes the closest distance in km to the fault plane, and P is zero for 50 percentile values and one for 84 percentile values. The expression of D was determined so that a peak ground acceleration becomes independent of magnitude at the fault surface. The term of ChH was introduced because it fairly raised the multiple correlation coefficient in the case of PGA (Ref.5). The coefficients for the peak ground motions are listed in Table 3. The relations between the coefficients and the natural periods for the acceleration response spectra are shown in FIg.4. The fraction of critical damping is 5%. Intensities of ground motions from earthquakes at each magnitude, distance and depth are assumed to be lognormally distributed with standard deviation Cp in log-intensity. In the subsequent analysis the distribution of intensities is truncated at $\pm$ 2.6 Cp from the median value. The equations above can be applied to the site where the surface Vs is between 300 and 600m/s.

Table 3 Coefficients of attenuation equations for predicting peak horizontal ground motions.

	Cm	Ch	Cd	Co	Cp
ACCELERATION (cm/s^2)	0.627	0.00671	2.212	1.711	0.211
VELOCITY (cm/s)	0.795	0.00550	2.065	-0.607	0.212
DISPLACEMENT (cm)	1.023	0.00372	1.967	-0.765	0.230

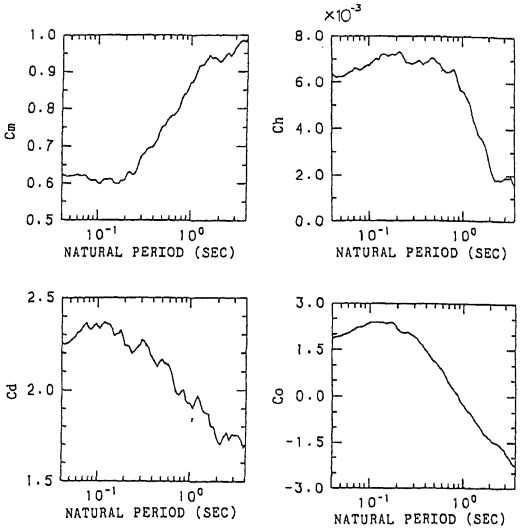

Fig.4 Variation of coefficients with natural period for the attenuation equation of acceleration response spectra.

CALCULATION OF SEISMIC HAZARD CURVE

By combining the earthquake occurrence model and the attenuation model above, we can calculate a seismic hazard curve for any site in the Kanto district. The equations used for the calculation are

$$\nu = \sum_{i=1}^{r} \sum_{j=1}^{mi} Fi(Mj) \left(\sum_{k=1}^{Nij} P(Y>y; Mj, Rk, Hk) / Nij \right)$$

$$Mj = (Mmin)i + \Delta M\,(j-1) \qquad (5)$$

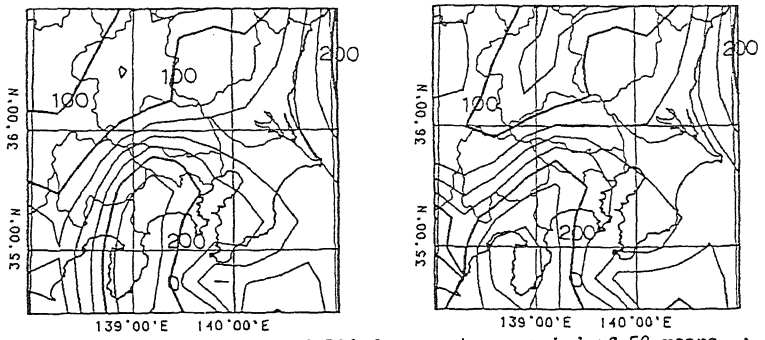

Fig.5 Contour maps of expected PGA for a return period of 50 years : (left) long-term hazard map. (right) instantaneous hazard map. Numerals denote PGA in cm/s^2.

where ν is the mean occurrence times during T years that the maximum intensity at the site, Y, will exceed a value y, Fi(Mj) is the expected number of earthquakes with magnitude Mj in the seismic source zone i during the period, (Mmin)i is the minimum magnitude in the zone i, ΔM is taken as 0.1, Nij is the number of ways that the fault plane of earthquakes with magnitude Mj can be located on the seismic source zone i, and P (Y>y; Mj, Rk, Hk) is the probability that intensity y will be exceeded when the k-th earthquake having the magnitude Mj, the closest distance Rk, and the depth Hk will occur.

For an estimate of long-term stationary seismic hazard, Fi(Mj) is derived by a Poisson model of earthquake occurrence. For an estimate of instantaneous seismic hazard, Fi(Mj) is derived by the stochastic time-predictable model. The probability q of the intensity exceeding y at the site during T years is given by

$$q(y) = 1 - \exp(-\nu). \qquad (6)$$

The return period of y is defined as $1/\nu$ and the probability density function of maximum intensity is obtained by differentiating q.

RESULTS

Figure 5 shows the contour maps of expected PGA for a return period of 50 years. The left is the long-term hazard map based on Poisson process. The right is the instantaneous hazard map during the next 50 years from the present(A.D.1988) based on the stochastic time-predictable model shown in Fig.3. The expected PGAs are highest near the Izu peninsula and lowest in Gunma prefecture in both maps. The expected PGAs in and around zone 6 are larger in the instantaneous hazard map than in the long-term hazard map. This reflects the high probability of earthquake occurrence in zone 6 in the near future.

For each site more information can be obtained. For example, some of the result for a reference site (139°40'E,30°40'N) in the eastern Tokyo are shown in Figs.6~8. Figure 6 shows the probability density curves of maximum PGA during 50 years. The instantaneous hazard curve moves slightly to the lower side of PGA compared with the long-term hazard curve because the large earthquake in zone 4 is expected not to occur in the next 50 years as shown in Fig.3. The expected PGA for a return period of 50 years is 186 cm/s^2 from the long-term hazard curve and 171 cm/s^2 from the instantaneous hazard curve. Figure 7 shows the relative frequency distribution of seismic source zones for the earthquakes whose PGAs exceed 186 cm/s^2 in the case of the long-term hazard estimation. The numbers correspond to those in Table 1. The contributions of large earthquakes in zone 4 and moderate earthquakes in zones 22,23 and 24 are large. This result may be useful for generating strong motions based on the probabilistic seismic hazard analysis. Figure 8

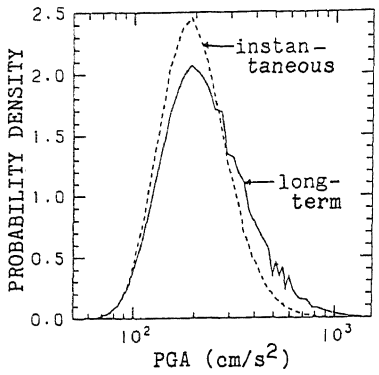

Fig.6 Probability density curves of PGA during 50 years for the site in the eastern Tokyo.

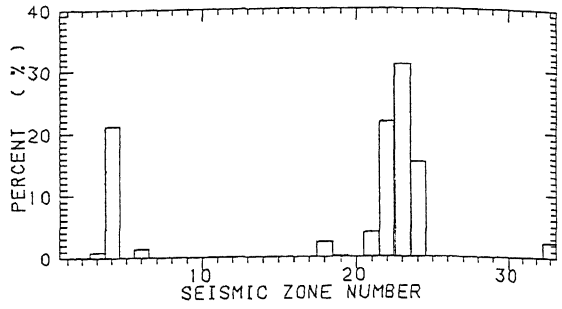

Fig.7 Relative frequency distribution of seismic source zones for the earthquakes whose PGAs exceed 186 cm/s^2.

shows the uniform risk acceleration response spectra for three return periods in the case of the long-term hazard estimation. The spectra may be used for generating strong motions.

CONCLUSIONS

A probabilistic model for seismic hazard estimation in the Kanto district was proposed. The effect of focal depths, which was not fully investigated in the past, was taken into account in the model. The effect of fault extent and the recurrence nature of large earthquakes can be included. It will be necessary to revise the partition of seismic source zones, the seismicity parameters for each zone, and the attenuation equations for the intensities of ground motions by further investigations on them.

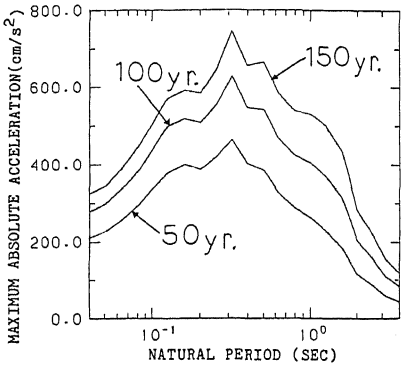

Fig.8 Long-term uniform risk acceleration response spectra for the site in the eastern Tokyo.

REFERENCES

1. Schwartz, D.P. and K. J. Coppersmith, Fault behavior and characteristic earthquakes : examples from the Wasatch and San Andreas Fault Zones, J.Geophys.Res., 89, 5681-5698, (1984)
2. Wesnousky,S.G., C.H.Scholz, K.Shimazaki, and T.Matsuda, Integration of geological and seismological data for the analysis of seismic hazard : a case study of Japan, Bull.Seism.Soc.Am., 74, 687-708, (1984).
3. Blume, J.A., "Diablo Canyon Nuclear Power Plant : Probabilities of peak site Accelerations and Spectral Response Acceleration from Assumed Magnitudes up to and Including 7.5 in all Local Fault Zones", report D-LL 11 prepared for Pacific Gas & Electric Company, May 27, (1977).
4. Anagnos, T. and A.S. Kiremidjian, Stochastic time-predictable model for earthquake occurrences, Bull.Seism.Soc.Am., 74, 2593-2611, (1984).
5. Annaka,T., A.Yamaya, H.Momobayashi, and Y.Nozawa, A study on the attenuation functions of peak horizontal ground accelerations at design base layer from the observed records obtained at the TEPCO's stations in and around the Kanto district, Proc. of Symp. on Earthquake Engineering Reserch, 129-132, (1987). (in Japanese)